Heliyon 9 (2023) e18162

Contents lists available at ScienceDirect

Heliyon

journal homepage: www.cell.com/heliyon

Nanocomposite with high adsorption activity developed using stabilized silver modified alumina and TiO_2-NPs incorporated into β-cyclodextrin-graphene oxide

Nafiseh Einafshar [a], Hamed Amiri Farmad [b], Seyed Mostafa Moshirian Farahi [c], Elham Einafshar [c,d,*]

[a] Faculty of Civil Engineering, Quchan University of Technology, Quchan, Iran
[b] Department of Pharmaceutical Biotechnology, School of Pharmacy, Mashhad University of Medical Sciences, Mashhad, Iran
[c] Department of Pharmacology, Faculty of Medicine, Mashhad University of Medical Sciences, Mashhad, Iran
[d] Pharmaceutical Research Center, Pharmaceutical Technology Institute, Mashhad University of Medical Sciences, Mashhad, Iran

ARTICLE INFO

Keywords:
Methylene blue
Combustion synthesis
Adsorption
Graphene oxide
Purification

ABSTRACT

Multifunctional nanocomposites $Ag/Al_2O_3/TiO_2$@β-cyclodextrin-graphene oxide (AATG) incorporating graphene oxide sheets, TiO_2, and Ag/Al_2O_3 nanoparticles were prepared in two steps. We benefited from the inherent properties of β-cyclodextrin to create a stable aqueous graphene solution capable of self-assembling in situ grown TiO_2 nanoparticles on graphene nanosheets. Ag/Al_2O_3 catalysts with a high surface-to-volume ratio were prepared by a combustion technique in solution with urea as a new fuel. The synthesized nanoparticles were also characterized by X-ray diffraction (XRD), Brunauer-Emmett-Teller (BET) surface analysis, and BJH pore analysis. FE-SEM was used to evaluate the morphology of β-cyclodextrin-graphene oxide, Ag/Al_2O_3 and AATG nanoplatforms. This research examined the use of AATG as a novel nanocomposite for removing methylene blue from water and compared its effectiveness with that of TiO_2@β-cyclodextrin-graphene oxide (TG) as an intermediate material to assess the impact of the final composite and its components on absorption. The effect of pH, temperature, time, and dye concentration on the reaction rate was investigated. The results showed that at pH above 4, the adsorption rate of MB by AATG gradually increased to about 98%. The results also show that methylene blue is more effectively removed at higher temperatures, implying that the adsorption is temperature dependent and the elimination process is endothermic. The adsorption kinetics, isothermal studies, and thermodynamic analysis were also evaluated. The adsorption data showed excellent agreement with pseudo-second order models ($R^2 > 0.99$) and the Langmuir isotherm.

The AATG nanocomposites showed excellent adsorption activity, making them potential candidates for water treatment.

1. Introduction

With increasing concern for the safety of drinking water, there is a growing need for efficient methods to remove contaminants such as toxic organic pollutants and pathogenic bacteria from wastewater [1,2]. In the field of environmental protection, industrial

* Corresponding author. Mashhad University of Medical Sciences, Mashhad, P.O. Box: 91779-48564, Iran.
E-mail address: EinafsharE4001@mums.ac.ir (E. Einafshar).

https://doi.org/10.1016/j.heliyon.2023.e18162
Received 11 June 2023; Received in revised form 1 July 2023; Accepted 10 July 2023
Available online 11 July 2023

wastewater poses a major challenge. Aromatic dyes have a relatively stable chemical structure that is also resistant to degradation, which means that they are likely to cause severe contamination of drinking water and irrigation systems [3,4].

Among the various organic pollutants, methylene blue (MB) is one of the unsafe colored pollutants that are highly toxic and have carcinogenic effects [5]. Due to these toxic chemicals, environmental pollution has become a global problem. In contrast, bleached dye is relatively less toxic and almost harmless after degradation, while colored water is practically useless. When the dyed solution is bleached to produce colorless water, it can be used for washing, cooling, irrigation, and cleaning [6]. Most synthetic organic dyes are used in agriculture, textile, printing, leather, paper, cosmetics, food, and pharmaceutical industries. There are many physical and chemical methods for wastewater treatment, including adsorption, reverse osmosis, precipitation, chemical oxidation, ozonation, membrane filtration, and ion exchange [3,7]. Among the methods for dye removal, adsorption is the most commonly used and effective method that gives promising results [8].

Graphene and graphene oxide have a unique 2D structure and properties that make them unique among carbon-based materials [9]. Graphene oxide has the largest surface area, excellent thermal conductivity and optical transparency, superior charge carrier mobility, high chemical stability, great mechanical strength, flexibility and low production cost. It is an ideal carrier or promoter as well as a super platform adsorbent for organic dyes and heavy metal ions [10]. However, graphene sheets are difficult to disperse in aqueous media without functionalization. Therefore, the modification of graphene oxide is of great importance for the expansion of its practical application [11]. It has been demonstrated that supramolecular hybrids of nanosheets and graphene oxide conjugated with cyclodextrin provide high dispersibility in polar solvents. Cyclodextrins are ring-shaped materials with hydrophobic cavities inside and hydrophilic surfaces outside [12]. Therefore, it is possible to functionalize graphene oxide with cyclodextrin, which can act as a host-guest inclusion complex that carries various types of chemicals and organic molecules in its cavities. Wang et al. developed graphene oxide with β-cyclodextrin as an efficient MB and fuchsin acid remover due to host-guest interactions between the cyclodextrin and dye contamination [13]. In other studies, the conjugation of cyclodextrin on graphene oxide surfaces was found to be highly effective in the adsorption of heavy metal ions from water [11,14]. It is also possible to improve the adsorption capacity of graphene oxide by mixing it with efficient materials. Recent studies have combined nanoscale particles, such as nano titania nanoparticles and Ag/Al_2O_3 nanocomposite, with graphene oxide to remove MB dye. Due to its physical and chemical stability and larger surface area, nanoscale titanium oxide provides good mechanical strength to graphene oxide, as well as chemical resistance and adsorption capacity. TiO_2 has a synergistic effect by increasing the adsorption capacity due to charge interactions with the dye [15]. The activity of TiO_2 is significantly limited by the low electrical conductivity within the TiO_2 network. This problem may be overcome by combining TiO_2 with noble metals, such as Ag and Ag/Al_2O_3. Noble metal nanoparticles exhibit size-dependent optical, electrical, and catalytic properties, as well as surface plasmon absorption. Due to electron capture properties, noble metals deposited on TiO_2 surfaces can significantly enhance the activity and increase the charge transfer at the interface [16]. Alumina particles have a large specific surface area and are considered the most inert material in the vicinity of human organisms. They have shown satisfactory biocompatibility [17].

We have simultaneously produced alumina and silver nanoparticles using the solution combustion synthesis (SCS) process, which is a simple, rapid, and versatile method for producing various nanoscale materials [18,19].

The objective of this study is to optimize a method for preparing a new nanocomposite that exhibits adsorption activity towards MB. The nanoadsorption material was prepared by depositing silver-modified alumina and TiO_2 nanoparticles onto the smooth surface of β-cyclodextrin-graphene oxide. There are no previous reports on the simultaneous use of all these nanoparticles for the adsorption of MB from water. It is expected that the combination of TiO_2, Ag/Al_2O_3 and graphene oxide with their unique properties, will be an effective adsorbent for the removal of pollutants from wastewater. In the present work, we attempt to compare dye adsorption studies for TG and AATG. The adsorption equilibrium studies are carried out under different initial dye concentrations, adsorbent dosages and temperatures. The obtained data will be processed using adsorption kinetics and isothermal models, and the thermodynamic behavior of adsorption of cationic dyes will also be evaluated. Further studies are needed to comprehensively investigate other properties of this nanocomposite, including its photocatalytic properties for pollutant decomposition or antibacterial properties.

2. Materials and methods

2.1. Materials

Graphite powder, β-cyclodextrin, anatase TiO_2 powder with a particle size of 25 nm, urea, and 4-dimethylaminopyridine (DMAP) were purchased from Sigma Aldrich. Hydrogen peroxide (H_2O_2, 30%), sulfuric acid (H_2SO_4), potassium permanganate ($KMnO_4$), sodium nitrate ($NaNO_3$), aluminum nitrate nonahydrate ($Al(NO_3)_3.9H_2O$), silver nitrate ($AgNO_3$; 99.5%), and MB were from Merck Co. Fluka provided 1-ethyl-3-(3-dimethyl aminopropyl) carbodiimide hydrochloride (EDC). Deionized water was used throughout the experiment.

2.2. Synthesis of β-cyclodextrin-graphene oxide

Based on Hummers' method, graphene oxide was prepared from natural graphite [1]. The simple method to synthesize β-cyclodextrin-graphene oxide was carried out by the esterification of the carboxyl functional group of graphene oxide with the hydroxyl groups of β-cyclodextrin using EDC/DMAP, alluding to a previously described procedure [20,21]. A typical procedure consists of dispersing graphene oxide (0.03 gr) in 7.0 mL ultrapure water and then dissolving EDC (0.15 gr) as a coupling agent. After stirring for 45 min, DMAP (0.03 gr) and β-cyclodextrin (0.3 gr) were added. The mixture was stirred at room temperature for two days (RT). After

washing with deionized water, centrifugation at 14000 rpm for 10 min, and lyophilization of the remaining solid, the product was ready for use.

The accuracy of the synthesis and evaluation of the binding rate of cyclodextrin to graphene oxide was checked by Fourier-transform infrared spectroscopy and thermogravimetric analysis.

2.3. Synthesis of Ag/Al_2O_3 nanoparticles

As previously reported, Ag/Al_2O_3 nanocomposite was synthesized using solution combustion and urea as fuel [19]. The silver-promoted materials were prepared by dissolving an appropriate amount of $AgNO_3$ (1.56 gr) and $Al(NO_3)_3.9H_2O$ (7.36 gr) in DI

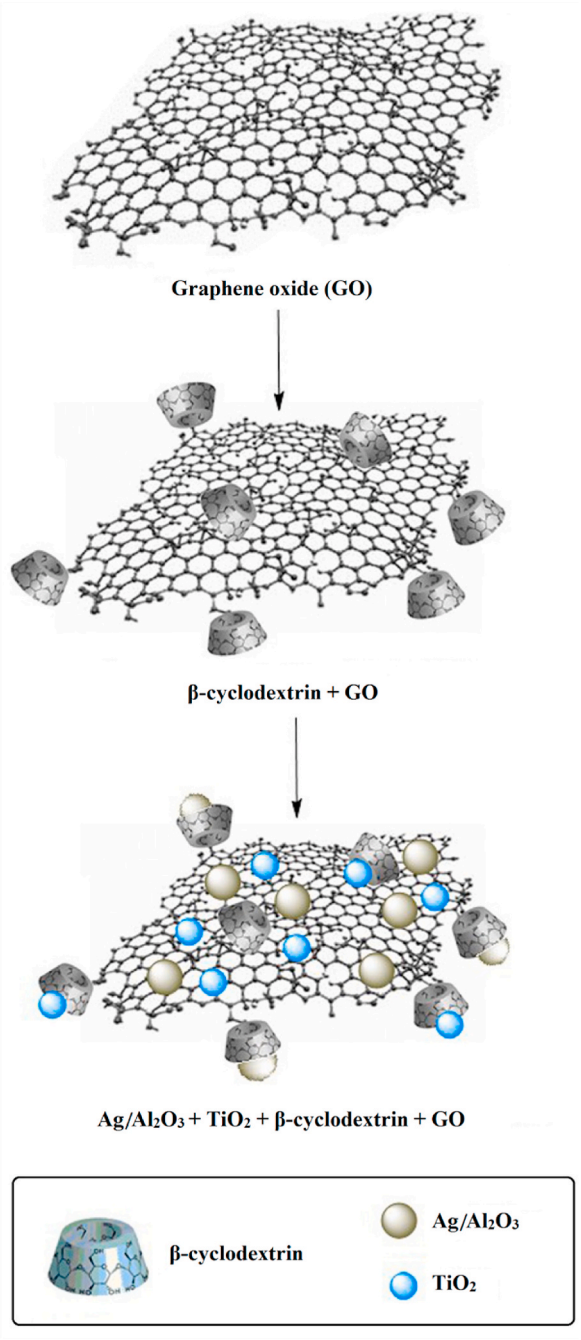

Fig. 1. Schematic of the synthesis of AATG nanocomposite.

water and using urea (3.49 gr) as a combustion fuel. The use of urea resulted in the production of Ag/α-alumina. After the solution was stirred, it was placed in a furnace for 30 min at different temperatures (400 and 500 °C) and then calcined at 900 °C for 1 h. It was found that this particular process provided sufficient heat of combustion to produce Ag/Al_2O_3 nanocomposites.

2.4. Synthesis of $Ag/Al_2O_3/TiO_2$@β-cyclodextrin-graphene oxide (AATG) nanocomposite

A two-phase method for the synthesis of AATG nanocomposites was developed. We dispersed (0.05 gr) β-cyclodextrin-graphene oxide in 10 mL DI water under sonication for 1 h. The (0.01 gr) TiO_2 and (0.01 gr) Ag/Al_2O_3 nanoparticles (with equal weight) were mixed with 5 mL toluene and added to the aqueous β-cyclodextrin-graphene oxide solution. Then the TiO_2 and Ag/Al_2O_3 nanoparticles were allowed to stir for 12 h to ensure that they coordinated with the β-cyclodextrin-graphene oxide layers. The AATG nanocomposites were precipitated by adding acetone and centrifugation. Residual materials were removed by washing the nanocomposites with THF. The final AATG nanocomposites were freeze-dried and stored dry until use.

Fig. 1 shows a schematic representation of the synthesis process for the final AATG nanocomposites.

2.5. Characterization

The FTIR spectra of the different samples were measured with an FTIR spectrometer (Bruker, USA). The morphology of the samples was determined with FE-SEM using a Mira III FEG (TESCAN, London, UK, Ltd). The surface area was calculated using Brunauer-Emmett-Teller (BET). An analysis of BET using MicroActive for TriStar II Plus version 2.03. Barret-Joyner-Halenda (BJH) models were then used to measure the pore sizes of β-cyclodextrin-graphene oxide and Ag/Al_2O_3 nanoparticles. Further TGA-DTA (thermogravimetric analysis) was performed using a TGA instrument (model TGA 50, Shimadzu, Japan) under air atmosphere at RT up to 800 °C with a heating rate of 10 °C/min. The absorbance values were recorded using a UV–Vis spectrophotometer (Varian CARY 100, California, USA) to determine the MB concentration. The Ag/Al_2O_3 was also analyzed using D8-Advance Bruker Cu K_α ($\lambda = 0.15406$ nm) X-ray diffraction (XRD).

2.6. Adsorption of organic pollutants

The amount of adsorbed MB on AATG and TG composites was determined by adding 1 mg of each compound to 20 ppm MB solutions. After centrifugation at 12000 rpm for 5 min, unreacted materials were filtered out. Quantitative analysis was performed by measuring the absorbance of the filtered solution at the maximum wavelength of 665 nm and determining the absorbance capacity of the dye MB using equation (1) and 2 [22]:

$$\text{Adsorption } (\%) = C_0 - C_t \,/\, C_0 \ * 100 \tag{1}$$

$$Q = C_0 - C_e * V \,/\, m \tag{2}$$

C_0 is the absorbance of the dye at time zero, C_t ($mg.L^{-1}$) is the absorbance of the dye at time (t), V is the volume of the solution (L), and m is the mass of the adsorbent (gr).

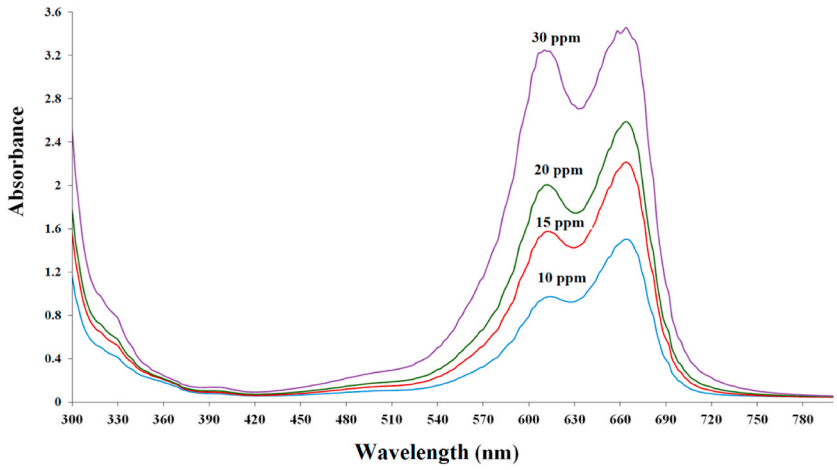

Fig. 2. UV–Vis spectra of MB dyes at different concentrations.

3. Results and discussion

3.1. Characterization

MB absorption spectra at different concentrations are shown in Fig. 2. Peaks at 300 nm confirm the presence of an aromatic ring, while peaks at 600–700 nm indicate the absorption of the conjugated π-π structure.

The phase composition of the nanopowders was investigated using XRD analysis. To measure the crystallite size, the strongest peaks in the XRD patterns of Ag/Al_2O_3were filtered out using the Scherrer formula ($D = 0.9\lambda/\beta.Cos\theta$), where D is the crystal size, λ is the X-ray wavelength, θ is the Bragg angle, and β is the peak broadening [18]. Fig. 3 shows different XRD patterns for the synthesis of Ag/Al_2O_3 nanocomposites at 400 and 500 °C. It was found that the crystallite size was 2.355 Å at 400 °C and 2.356 Å at 500 °C. The Ag phases were observed at 2θ of 38.2°, 44.3°, 64.5°, and 77.4°, corresponding to the lattice planes (111), (200), (220), and (311) of the face-centered cubic (fcc) structure of metallic silver in all samples. This observation could be due to the crystalline phase of Ag species on the Ag/Al_2O_3 [18,23]. The formation of Ag nanoparticles dispersed in thin Al_2O_3 films was confirmed by these results [24,25]. The XRD data yielded peaks that also confirmed the presence of α-Al_2O_3, as in 2 theta angles of 35.1° corresponding to (104) [26].

XRD is not the optimal technique for characterizing β-cyclodextrin-graphene oxide due to potential interference from β-cyclodextrin, which could affect the XRD analysis of graphene oxide. This interference results in a reduction in the characteristic peak intensity associated with the graphene oxide sheets, making it difficult to identify the diffraction peak in the XRD pattern. The presence of β-cyclodextrin, a cyclic oligosaccharide, can disrupt the orderly stacking of graphene oxide layers on a micrometer scale and lead to disorder in the arrangement of carbon atoms within those layers [27]. Therefore, complementary analytical techniques were utilized to confirm the synthesis of β-cyclodextrin-graphene oxide.

The FTIR spectra of graphene oxide, β-cyclodextrin-graphene oxide, and the prepared nanocomposites were investigated (Fig. 4). All samples exhibited peaks at 3424 , 1720 and 1380 cm^{-1} as the stretching vibration adsorption peaks of hydroxyl, carboxyl and carbonyl groups in graphene oxide, respectively, and the band at 1583 cm^{-1} was attributed to C═C stretching mode of the sp^2 hybridization carbons of skeletal network. Additionally, the peaks at 1055 and 1230 cm^{-1} were indicative of the stretching vibrations of the epoxy groups [28]. To confirm the synthesis of β-cyclodextrin-graphene oxide composites, FTIR of the composite was performed. The peak at 2925 cm^{-1} appeared to correspond to the asymmetric C–H stretching vibration. The peaks at 1030 and 942 cm^{-1} corresponded to the antisymmetric glycosidic (C–O–C) vibrations and the R-1, 4-bond framework vibration of cyclodextrin, respectively. All characterized bands confirmed the successful synthesis of the β-cyclodextrin-graphene oxide composite [29]. The FTIR spectrum of the TG and AATG nanoparticles shows a broad peak at 550-800 cm^{-1} caused by the Ti–O–Ti band. The peak at 3400 cm^{-1} confirmed the presence of hydroxyl groups on the surface and the peak at 1626 cm^{-1} was assigned to the vibrations of OH bonds on the surface of TiO_2 [30]. A broad peak at 400-1000 cm^{-1}, indicated the characteristic peaks confirming the presence of Al_2O_3 in composite. For the Al_2O_3 NPs, the characteristic peaks in the FT-IR spectra near 3300-3400 cm^{-1} and 1628 cm^{-1} indicate the stretching vibration and the bending vibration of the hydroxyl group peaks on the surface of the Al_2O_3 particles, respectively. Both bands confirm the presence of physically absorbed water molecules [31].

The thermal stability of an adsorbent is a critical factor affecting its application. The thermal stability of β-cyclodextrin-graphene oxide was investigated using TGA. Fig. 5 shows the TGA curves and the corresponding derived weight loss (DTA) curves for graphene oxide, β-cyclodextrin-graphene oxide and Ag/Al_2O_3. When the temperature is below 100 °C, graphene oxide loses a little weight (~17%), which is mainly due to the evaporation of water. The rapid weight loss of graphene oxide started at 200 °C and mass equilibrium was reached at 500 °C. The mass loss (~72%) could be mainly due to pyrolysis of the oxygen-containing groups.

Rapid mass loss occurred only at temperatures above 200 °C, indicating that the prepared graphene oxide has reasonable thermal stability at lower temperatures, which seems to be sufficient for most wastewater treatment requirements [32]. Additionally, we should mention that the energy required to evaporate the solvent and remove the oxidation products from graphene is completely different from the heat required to remove the added organic groups on graphene. Therefore, the amount of cyclodextrin, grafted onto graphene oxide, can be calculated by this method. In addition, the amount of β-cyclodextrin grafted onto graphene oxide was calculated to be 36 wt% based on the thermal decomposition [27]. The DTA curves of the Ag/Al_2O_3 powder showed an endothermic

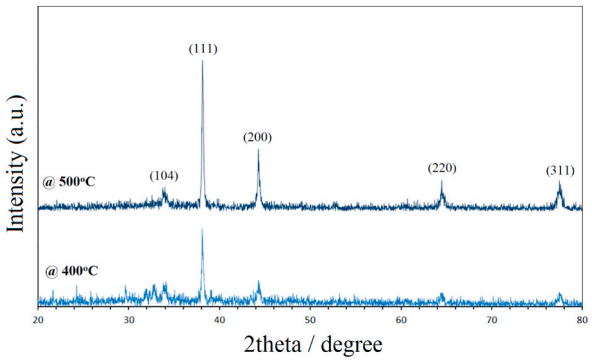

Fig. 3. the XRD patterns of Ag/Al_2O_3 nanocomposites at different temperatures.

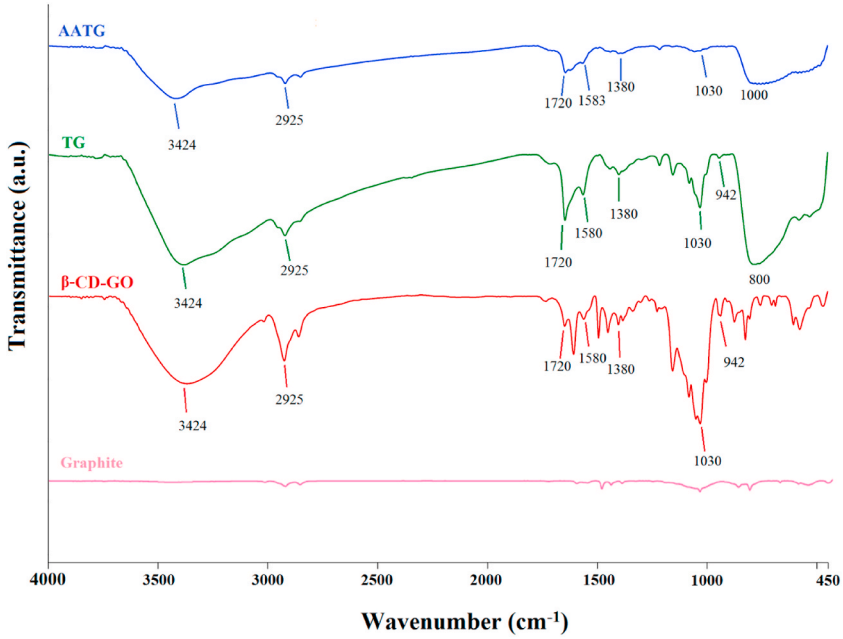

Fig. 4. The FTIR spectra of graphite, β-cyclodextrin-graphene oxide, TG and AATG.

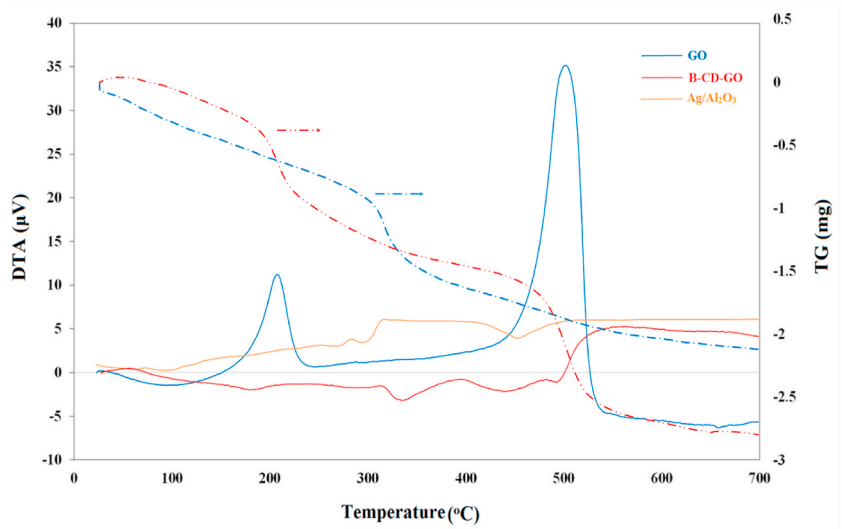

Fig. 5. The TGA/DTA analysis of graphene oxide, β-cyclodextrin-graphene oxide and the DTA analysis of Ag/Al_2O_3.

peak at 120 °C related to water evaporation. The exothermic peak found at about 270 °C could be caused by the decomposition and combustion of organic molecules. The exothermic peak at about 380 °C could be due to the formation of Ag particles, while the broad peak at 520 °C could be related to the formation of Al_2O_3. Taken together, the results indicate that the organic components of the films were completely eliminated before the formation temperature of the Ag/Al_2O_3 nanoparticles was reached [24].

This particular surface area is an important parameter for an adsorbent that directly affects adsorption performance. A larger

Table 1
Surface properties of Ag/Al_2O_3 and β-cyclodextrin-graphene oxide samples.

Sample	BET surface area ($m^2.g^{-1}$)	Total pore volume ($cm^3.g^{-1}$)	Pore diameter $BJH_{(nm)}$
Ag/Al_2O_3	3.7796	0.016000	3.12
β-cyclodextrin-graphene oxide	22.0871	0.067877	9.88

surface area provides more adsorption sites on the surface, thus increasing the adsorption efficiency. We used the BET method to measure the surface area, while the pore size (pore diameter and volume) was measured using the BJH method [30]. The specific surface area of β-cyclodextrin-graphene oxide and Ag/Al_2O_3 were 22.087, and 3.779 $m^2\ g^{-1}$, respectively, and the total pore volumes were 0.06787 and 0.01600 $cm^3.g^{-1}$ for β-cyclodextrin-graphene oxide and Ag/Al_2O_3, respectively (Table 1). The BET measurements reveal that the values for β-cyclodextrin-graphene oxide are comparatively lower than those reported in the literature for graphene oxide [33]. The presence of β-cyclodextrin molecules on the surface of graphene oxide may change the chemistry and properties of the surface, affect the absorption of gases, and lead to a decrease in BET values. On the other hand, the small size and the presence of many pores in the synthesized nanocomposite promise better performance as an absorbent.

The FE-SEM analysis was used to evaluate the morphology of nanocomposites. The FE-SEM image of the β-cyclodextrin-graphene oxide (Fig. 6A) showed uniform spherical shapes on the smooth surface, indicating the presence of cyclodextrin on the graphene oxide sheets. Fig. 6B showed the morphology of Ag/Al_2O_3, where the larger particles were probably Al_2O_3 powders, while the smaller bright particles represented the Ag powders. The morphology analysis of the AATG powders indicated a complete coverage of the graphene oxide surface by particles of titanium oxide and silver oxide and Alumina (Fig. 6C). The AATG nanocomposites possessed a narrow poly-dispersity index and the obtained mean diameter of the particle size was about 30 ± 7.7 nm (Fig. 6D).

3.2. Effect of the contact time

The contact time is one of the most important parameters for the successful use of the adsorbent for practical application. MB adsorption rates on the AATG composite were measured under the conditions (the reaction temperature is 25 °C and the concentration of adsorbent is (0.4 g L^{-1}) and primary MB (20 mg L^{-1}). We measured the adsorption of MB over a range of times from three to Half-hour.

Based on the data presented in Fig. 7, it can be observed that the adsorption process has a rapid adsorption rate within the first 5 min and that equilibrium is reached after about 30 min, with no time-dependent change in the amount of adsorbed dye. Overall, more than 99% of MB on the AATG composite was removed within the first 5 min. The researches results show that the removal efficiency of β-cyclodextrin-graphene oxide is 20% higher than that of graphene oxide, increasing from 70% to 90% in 60 min. However, the new nanocomposite has achieved a removal rate of up to 99% in less than 30 min. This is due to the fact that adsorption on graphene oxide occurs mainly on its two-dimensional surface, whereas on β-cyclodextrin-graphene oxide it occurs both on the surface of the graphene

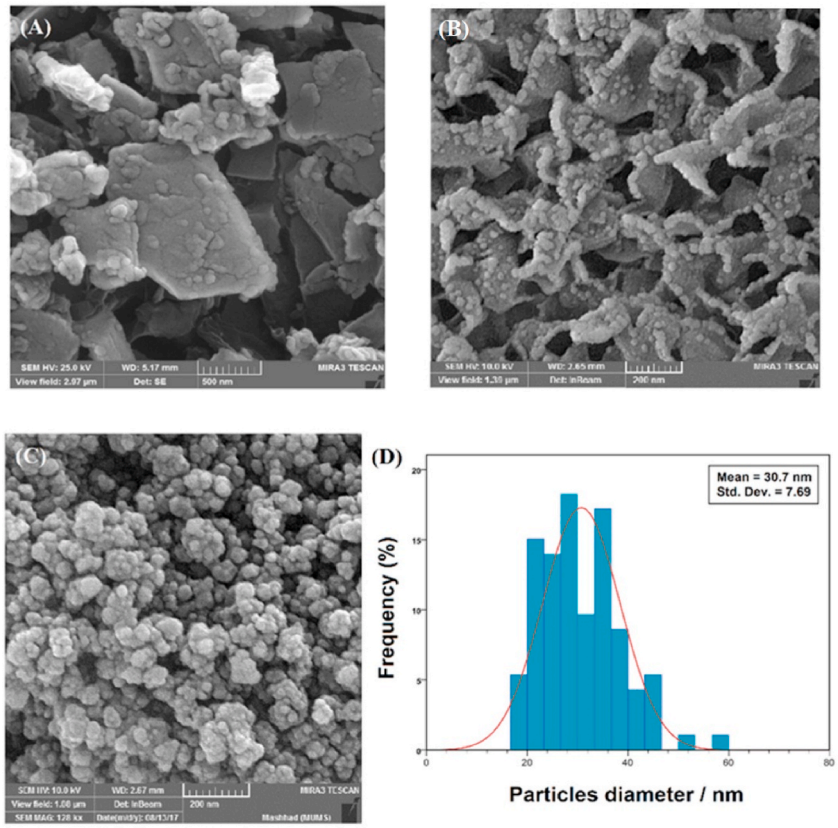

Fig. 6. FE-SEM images of β-cyclodextrin-graphene oxide (A), Ag/Al_2O_3 (B) and AATG nanocomposite (C), and particle size distribution of AATG (D).

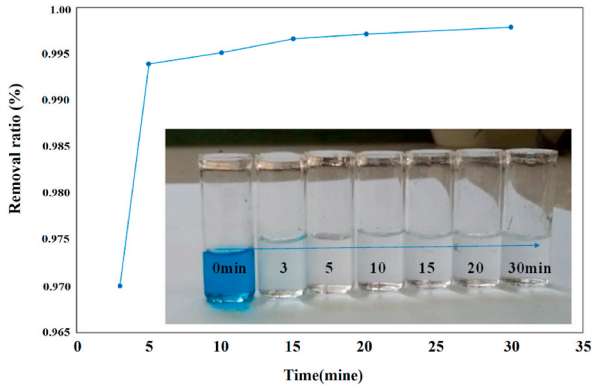

Fig. 7. Effect of time on MB adsorption onto the AATG.

oxide nanosheets and on the shells of the cyclodextrin rings [11]. In addition, the improvement of the surface of β-cyclodextrin-graphene oxide by nano compounds that have a high surface-to-volume has also increased absorption. The sorption process consisted of two steps: a fast initial phase due to the adsorption of the MB dye on the surface of the composite, and a second step corresponding to the internal diffusion of the MB dye into the pores of the composite. Therefore, the equilibrium time was set at 30 min for all other experiments.

3.3. Effect of pH

In the purification of industrial wastewater, pH plays a critical role [34]. The pH of the aqueous solution is an important factor for the reaction rate. Different pH can affect not only charge transfer and detachment of surface functional groups, but also ionization, host-guest interactions, and catalyst reactions [35]. We investigated the effect of pH on the adsorption of MB at 25 °C on the AATG composite in a pH of 2–10. Hydrochloric acid (HCl) and sodium hydroxide (NaOH) were added to adjust the pH. Adsorption of MB at a concentration of 20 mg L^{-1} was enhanced by increasing the pH of the solution. Above pH 4, the adsorption rate of MB gradually increased by about 88%, while the pH remained stable up to pH 10 and the removal efficiency was stable at 98% (Fig. 8). Since TiO_2 and the surface of the composite are negatively charged and methylene blue has a cationic color, the adsorption is more effective at higher pH values [36]. Based on the results obtained, pH 6–10 was the optimal range for the elimination of MB.

3.4. Effect of temperature

To analyze the effect of temperature on the level of adsorption capacity, four different temperatures were studied (Fig. 9).

The results indicate that MB is more effectively removed at higher temperatures, which means that the adsorption is temperature dependent and the elimination process was endothermic, possibly due to the increased mobility of the dye at higher temperatures, so that a large number of molecules could obtain enough energy to interact with the available binding sites on the adsorbent [37].

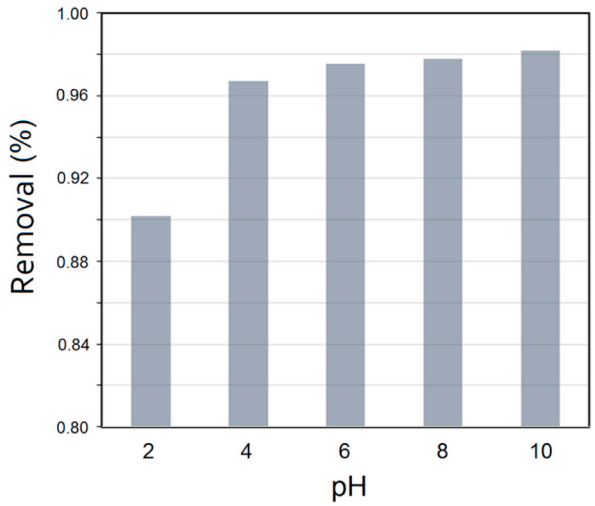

Fig. 8. The effects of pH in the initial solution on the adsorption of MB.

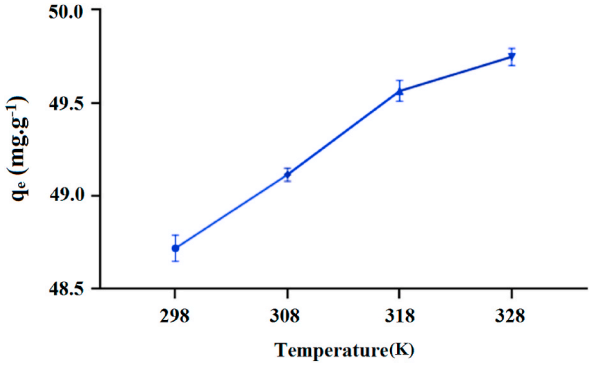

Fig. 9. The effect of temperature on adsorption amount of MB on the AATG.

3.5. Adsorption kinetics

Kinetics was investigated to determine the order of the rate constant and to define the dynamics of the adsorption process. Two different kinetic models were used to interpret the process of dye adsorption on the AATG surface (Fig. 10). According to the pseudo-first-order kinetic model, the occupation rate of adsorption sites depends on the number of vacancies. However, the pseudo-second-order kinetics assumes that the adsorption rate is controlled by the chemical adsorption mechanism and chemical adsorption involves the exchange of electrons between adsorbate and adsorbent.

The kinetic models of absorption include the pseudo-first-order and pseudo-first-order models shown in equations (3) and (4), respectively.

Pseudo-first-order model:

$$\mathrm{Log}\ (q_e - q_t) = \log q_e - \mathrm{KT} \tag{3}$$

Pseudo-first-order model:

$$t / q_t = 1 / k_2 q_e^2 + t / q_e \tag{4}$$

Where q_e and q_t represent the adsorption capacity of MB (mg.g^{-1}) at equilibrium and at a given time, t is the adsorption time (min), while k_1 (min^{-1}) and k_2 (g.mg^{-1}. min^{-1}) refer to the rate constants of the pseudo-first and pseudo-second order models, respectively [38]. Table 2 summarizes the kinetic constants obtained by linear regression for the two mentioned models. For the pseudo-first order kinetics, R_2 was 0.819 and 0.811, while for the pseudo-second order model it was 1 and 1 for AATG and TG, respectively. Based on the obtained results, the pseudo-second order model could better explain the adsorption of MB on AATG and TG. Since the pseudo-first order equation does not fully reflect the range of contact times, it is best suited for the onset of the adsorption process. Therefore, the pseudo-second order model can better describe the adsorption process from MB to AATG than the pseudo-first order model. It became clear that the adsorption process was controlled more by chemical actions than by mass transfer.

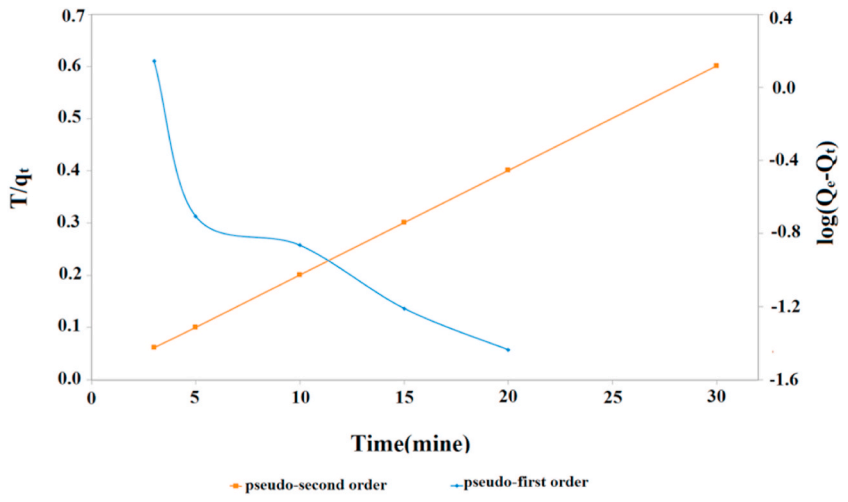

Fig. 10. Pseudo-first-order and pseudo-second-order kinetics of the MB adsorption onto the AATG.

Table 2
Parameters affecting pseudo-first and second-order kinetic models.

kinetic Models	Pseudo-first-order			Pseudo-second-order		
parameter	Rate constant $K_1(min^{-1})$	q_e ($mg.g^{-1}$)	R^2	Rate constant $K_2(g.mg.min^{-1})$	q_e ($mg.g^{-1}$)	R^2
AATG	0.033	−4.147	0.819	0.336	49.751	1
TG	0.015	−0.198	0.811	0.200	50.000	1

3.6. Adsorption isotherms

A study of isotherms shows how the adsorbate interacts with the adsorbents and represents the key parameter for the optimization of an adsorption system [39]. Langmuir and Freundlich isotherms are two models commonly used to calculate adsorption isotherms. According to the Langmuir isotherm model, adsorption occurs over homogeneous monolayer surfaces with independent adsorption energies. It also indicates that there is no interaction between the adsorbed molecules. In Freundlich isotherm, adsorption occurs over monolayers (chemisorption) and multilayers (physical sorption), and the adsorbate is adsorbed on the heterogeneous surface with different energies [39].

Equations (5)–(7) represent the Henry, Langmuir, and Freundlich isotherm adsorption models, respectively.

Henry's equation:

$$q_e = K_h\, C_e \tag{5}$$

Langmuir equation:

$$C_e \;/\; q_e = C_e/q_{max} + 1/q_{max} \tag{6}$$

Freundlich equation:

$$Ln\ q_e = \ln K_f + 1/n\ \ln C_e \tag{7}$$

Where q_m ($mg.g^{-1}$) would be the maximum adsorption capacity. K_H, K_L, and K_F are the constants associated with adsorption intensity and adsorption capacity. The parameters of Henry, Langmuir and Freundlich isotherm equation are shown in Table 3. The results indicated that the fitting degree of Langmuir isothermal model is much more acceptable than that of Freundlich and Henry isothermal model, which indicates that the adsorption of MB on AATG and TG is mainly a single layer adsorption process (Fig. 11). At the same time, the adsorption process is homogeneous. The Freundlich constant (1/n) is less than 1.0, indicating a favorable process. The comparative q_{max} calculation according to the Langmuir model shows that the modification of TG with Ag/Al_2O_3 increases the adsorption capacity. In comparison, the maximum adsorption capacity values of MB on other previously reported adsorbents are shown in Table 4.

When comparing the maximum adsorption capacity of MB on the β-cyclodextrin-graphene oxide adsorbent [11] to the AATG developed in this study, it can be observed that the two compounds have almost the same adsorption capacity. However, AATG reaches its maximum capacity in a shorter time (around 20 min), while it takes approximately 60 min for β-cyclodextrin-graphene oxide [11]. Therefore, the rate of absorption in the new absorbent is increased. Furthermore, due to the presence of titanium oxide and silver in the developed product, AATG has potential capabilities such as photocatalytic and antibacterial properties, which require further investigation in the future.

3.7. Adsorption thermodynamic

The information about spontaneity and natural energetic changes obtained by thermodynamic studies seems to be related to adsorption [38]. We studied the effect of different temperatures (298–338 K) on the adsorption of MB by AATG and TG composites and measured the following thermodynamic parameters according to equations (8) and (9):

$$\Delta G^0 = -\,RT\ Ln\ Kd \tag{8}$$

$$Ln\ Kd = -\Delta G^0 \;/\; RT = \Delta S^0 \;/\; R - \Delta H^0 \;/\; RT \tag{9}$$

Where R (8.314 J mol^{-1} K^{-1}) is the gas constant, T (K) is the absolute temperature in Kelvin, and K_d is the equilibrium constant. ΔS (J. mol^{-1}. K^{-1}) is the change in entropy, and ΔH ($kJ.mol^{-1}$) represents the change in enthalpy and ΔG ($kJ.mol^{-1}$) is the change in Gibbs free energy for a given process. The results of ΔS, ΔH and ΔG are shown in Table 5.

The value of ΔG was less than zero, indicating that the adsorption process was spontaneous. The value of ΔH was positive, indicating that the exothermic effect of MB adsorption was less than the endothermic effect of water solution desorption. The adsorption and removal efficiency of MB would increase with increasing temperature according to the theory. The ΔS was greater than zero, indicating that the molecules move rather randomly at the solution interface [46]. The data also show that the adsorption performance of MB dye on AATG is satisfactory. Sorption would be more efficient at higher temperatures because MB is readily dehydrated, resulting in more favorable sorption conditions.

Table 3
The comparison of parameters of three isotherm models affecting MB elimination through AATG and TG.

isotherm model	Henry		Langmuir			Freundlich		
parameter	K_h(L.mg^{-1})	R^2	q_m(mg.g^{-1})	K_L(L.mg^{-1})	R^2	K_F(mg^{1-n}.L^n.g^{-1})	n	R^2
AATG	2.905	0.439	72.993	2.537	0.997	46.163	4.56	0.512
TG	6.575	0.829	68.965	1.726	0.997	39.369	3.23	0.874

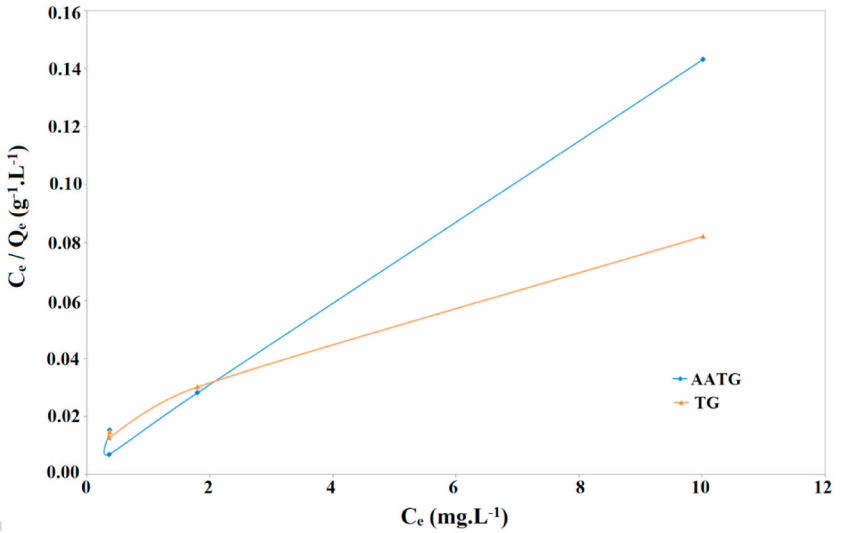

Fig. 11. Comparison of TG and AATG for the removal of MB by Langmuir isotherm model.

Table 4
A summary of maximum adsorption capacity of MB on various adsorbents.

Adsorbent	Conditions		q_{max} (mg.g^{-1})	Isotherm models	kinetic models	References
	pH	Temp				
Modified pumice with hydrochloric acid	10	298	15.87	L	PSO	[40]
MCM-41	5.86	303	47.79	F	PSO	[41]
C-HNTs	–	298	90.25	L	PSO	[42]
Moroccan Illitic Clay (MIC)	5	293	13.68	L	PSO	[43]
Olive Stone	7.2	–	13.20	L	PSO	[44]
brown algae Carolina	7	292	55	L	–	[45]
β-cyclodextrin/GO	–	303	76.4	L	PSO	[11]
AATG	5	298	72.993	L	PSO	current study
TG	5	298	68.965	L	PSO	current study

Table 5
The values of the three thermodynamic parameters.

Parameters	T (K)	ΔG^0 (KJ.mol^{-1})	ΔH^0 (KJ.mol^{-1})	ΔS^0 (J mol.K^{-1})
AATG	298	−0.793	0.6349	2.6656
	308	−0.820		
	318	−0.847		
	328	−0.873		
TG	298	−0.952	0.7838	3.1999
	308	−0.984		
	318	−1.016		
	328	−1.048		

4. Conclusions

Despite numerous studies on the use of graphene and other adsorbents, for the adsorption and degradation of dyes (especially MB), there is still potential for new contributions in the field.

In this study, Ag/Al_2O_3 composites were produced by a simple and fast combustion method. By incorporating this adsorption unit using β-cyclodextrin-graphene oxide conjugated with TiO_2, a highly efficient reagent for decolorizing water contaminated with MB was produced. The results presented here positively evaluate the increase in the efficiency of removal MB. The new adsorption production could be related to the excellent π-π interactions between graphene oxides and aromatic rings, which facilitated the adsorption of organic molecules such as MB. Several of operating parameters affected the adsorption process, including contact time, pH, initial dye concentration, and temperature. The adsorption capacity increased with increasing temperature. When the isotherms for the adsorption of the dye MB were analyzed, the isothermal Langmuir model was found to fit the data better. Based on the analysis of the adsorption kinetics data, the pseudo-second order model appears to be a good fit to the experimental data. The positive ΔH^0 indicates that the adsorption is endothermic. In this case, the negative ΔG^0 value indicates the feasibility and spontaneity of the adsorption process. The nanoparticles used in the nanocomposite are actually able to concentrate the substrate for photocatalytic degradation and antibacterial properties. More advantages in using this composite undoubtedly come from the extensive use of its properties, which make the long and laborious synthesis process appear economical.

Author contribution statement

Nafiseh Einafshar: Performed the experiments; Analyzed and interpreted the data, Wrote the paper.
Hammed Amiri Farmad: Analyzed and interpreted the data, Wrote the paper.
Seyed Mostafa Moshirian Farahi: Contributed reagents, materials, analysis tools or data, Wrote the paper.
Elham Einafshar: Conceived and designed the experiments; Analyzed and interpreted the data; Wrote the paper.

Data availability statement

Data will be made available on request.

Declaration of competing interest

The authors declare that they have no known competing financial interests or personal relationships that could have appeared to influence the work reported in this paper.

References

[1] L. Liu, H. Bai, J. Liu, D.D. Sun, Multifunctional graphene oxide-TiO2-Ag nanocomposites for high performance water disinfection and decontamination under solar irradiation, J. Hazard Mater. 261 (2013) 214–223.
[2] N. Madima, K.K. Kefeni, S.B. Mishra, A.K. Mishra, TiO2-modified g-C3N4 nanocomposite for photocatalytic degradation of organic dyes in aqueous solution, Heliyon 8 (2022), e10683.
[3] T.-J. Whang, M.-T. Hsieh, H.-H. Chen, Visible-light photocatalytic degradation of methylene blue with laser-induced Ag/ZnO nanoparticles, Appl. Surf. Sci. 258 (2012) 2796–2801.
[4] S.J. Salih, A.S.A. Kareem, S.S. Anwer, Adsorption of anionic dyes from textile wastewater utilizing raw corncob, Heliyon 8 (2022), e10092.
[5] H.u.A. Esra Altıntıg, M. Tuzen, A. Sarı, Effective removal of methylene blue from aqueous solutions using magnetic loaded activated carbon as novel adsorbent, Chem. Eng. Res. Des. 122 (2017) 151–163.
[6] H. Hassena, Photocatalytic degradation of methylene blue by using Al2O3/Fe2O3 nano composite under visible light, J. Mod. Chem. Chem. Technol. (2016), https://doi.org/10.4172/2329-6798.1000176.
[7] J. Saha, A. Begum, A. Mukherjee, S. Kumar, A novel green synthesis of silver nanoparticles and their catalytic action in reduction of Methylene Blue dye, Sustain. Environ. Res. 27 (5) (2017) 245–250.
[8] N.S. Ali, N.M. Jabbar, S.M. Alardhi, H.S. Majdi, T.M. Albayati, Adsorption of methyl violet dye onto a prepared bio-adsorbent from date seeds: isotherm, kinetics, and thermodynamic studies, Heliyon 8 (2022), e10276.
[9] V. Sharavath, S. Sarkar, D. Gandla, S. Ghosh, Low temperature synthesis of TiO2-β-Cyclodextrin–Graphene nanocomposite for energy storage and photocatalytic applications, Electrochim. Acta 210 (2016) 385–394.
[10] Y. Yang, E. Liu, H. Dai, L. Kang, H. Wu, J. Fan, X. Hu, H. Liu, Photocatalytic activity of Ag–TiO2-graphene ternary nanocomposites and application in hydrogen evolution by water splitting, Int. J. Hydrogen Energy 39 (2014) 7664–7671.
[11] Z. Yang, X. Liu, X. Liu, J. Wu, X. Zhu, Z. Bai, Z. Yu, Preparation of β-cyclodextrin/graphene oxide and its adsorption properties for methylene blue, Colloids Surf., B 200 (2021), 111605.
[12] Y.Z. Jie Yan, Fengxian Qiu, Hao Zhao, Dongya Yang, Jie Wang, Wenya Wen, Kinetic, isotherm and thermodynamic studies for removal of methyl orange using a novel β-cyclodextrin functionalized graphene oxide-isophorone diisocyanate composites, Chem. Eng. Res. Des. 106 (2016) 168–177.
[13] S. Wang, Y. Li, X. Fan, F. Zhang, G. Zhang, β-Cyclodextrin functionalized graphene oxide: an efficient and recyclable adsorbent for the removal of dye pollutants, Front. Chem. Sci. Eng. 9 (2015) 77–83.
[14] E. Einafshar, Z. Khodadadipoor, M. Nejabat, M. Ramezani, Synthesis, characterization and application of α, β, and γ cyclodextrin-conjugated graphene oxide for removing cadmium ions from aqueous media, J. Polym. Environ. 29 (2021) 3161–3173.
[15] H. Vardikar, B. Bhanvase, A. Rathod, S. Sonawane, Sonochemical synthesis, characterization and sorption study of Kaolin-Chitosan-TiO2 ternary nanocomposite: advantage over conventional method, Mater. Chem. Phys. 217 (2018) 457–467.
[16] Y.-W. Chen, D.-S. Lee, Photocatalytic destruction of methylene blue on Ag@ TiO2 with core/shell structure, Open Access Libr. 1 (2014) 1.
[17] V.A. Dubok, Bioceramics–yesterday, today, tomorrow, Powder Metall. Met. Ceram. 39 (2000) 381–394.
[18] Z. Naemi, M. Jafar-Tafreshi, M. Fazli, Studies on properties of AgAl2O3 nanocomposite synthesized by solution combustion technique under novel condition, J. Nanostru. 2 (2012) 183–189.

[19] E. Einafshar, Z. Khodadadipoor, M. Fazli, N. Einafshar, J. Mohebbi Zinab, S. Asaei, Preparation of Ag-Al_2O_3 nano structures by combustion method and investigation of photocatalytic activity, Int. J. Appl. Ceram. Technol. 18 (2021) 2064–2074.
[20] E. Einafshar, A. Haghighi Asl, A. Hashem Nia, M. Mohammadi, A. Malekzadeh, M. Ramezani, New cyclodextrin-based nanocarriers for drug delivery and phototherapy using an irinotecan metabolite, Carbohydr. Polym. 194 (2018) 103–110.
[21] E. Einafshar, A. Haghighi Asl, Azim Malekzadeh, M. Ramezani, Synthesis of new biodegradable nanocarriers for SN38 delivery and synergistic phototherapy, Nanomed. J. 5 (4) (2018) 210–216.
[22] Z. Ezzeddine, I. Batonneau-Gener, Y. Pouilloux, H. Hamad, Removal of methylene blue by mesoporous CMK-3: kinetics, isotherms and thermodynamics, J. Mol. Liq. 223 (2016) 763–770.
[23] N. Agasti, N. Kaushik, One pot synthesis of crystalline silver nanoparticles, J. Nanomater. 2 (2014) 4–7, https://doi.org/10.12691/ajn-2-1-2.
[24] C. Zhao, J. Du, D. Huang, Y. Li, J. Chen, W. Li, Microstructure and strong optical absorption property of the Ag/Al2O3 nano-films, J. Alloys Compd. 671 (2016) 419–423.
[25] T. Ivanova, A. Harizanova, T. Koutzarova, B. Vertruyen, Preparation and characterisation of Ag incorporated Al2O3 nanocomposite films obtained by sol-gel method, Cryst. Res. Technol. 47 (2012) 579–584.
[26] H.S. Kim, N.-K. Park, T.J. Lee, M.-H. Um, M. Kang, Preparation of nanosized α-Al2O3 particles UsingaMicrowave pretreatment atMild temperature, Adv. Mater. Sci. Eng. 2012 (2012) 6, https://doi.org/10.1155/2012/920105.
[27] H. Hu, J.H. Xin, H. Hu, X. Wang, X. Lu, Organic liquids-responsive β-cyclodextrin-functionalized graphene-based fluorescence probe: label-free selective detection of tetrahydrofuran, Molecules 19 (2014) 7459–7479.
[28] G.Z. Kyzas, E.A. Deliyanni, K.A. Matis, Graphene oxide and its application as an adsorbent for wastewater treatment, J. Chem. Technol. Biotechnol. 89 (2014) 196–205.
[29] V. Štengl, S. Bakardjieva, T.M. Grygar, J. Bludská, M. Kormunda, TiO2-graphene oxide nanocomposite as advanced photocatalytic materials, Chem. Cent. J. 7 (2013) 41.
[30] H. Mittal, S.S. Ray, A study on the adsorption of methylene blue onto gum ghatti/TiO 2 nanoparticles-based hydrogel nanocomposite, Int. J. Biol. Macromol. 88 (2016) 66–80.
[31] S. Mallakpour, M. Dinari, Enhancement in thermal properties of poly (vinyl alcohol) nanocomposites reinforced with Al2O3 nanoparticles, J. Reinforc. Plast. Compos. 32 (2013) 217–224.
[32] L. Cui, Y. Wang, L. Gao, L. Hu, Q. Wei, B. Du, Removal of Hg (II) from aqueous solution by resin loaded magnetic β-cyclodextrin bead and graphene oxide sheet: synthesis, adsorption mechanism and separation properties, J. Colloid Interface Sci. 456 (2015) 42–49.
[33] T. Jiang, W. Liu, Y. Mao, L. Zhang, J. Cheng, M. Gong, H. Zhao, L. Dai, S. Zhang, Q. Zhao, Adsorption behavior of copper ions from aqueous solution onto graphene oxide–CdS composite, J. Chem. Eng. 259 (2015) 603–610.
[34] Y. Huang, A.A. Keller, EDTA functionalized magnetic nanoparticle sorbents for cadmium and lead contaminated water treatment, Water Res. 80 (2015) 159–168.
[35] Y.L. Wang, S.P. Cui, X.K. Xu, M.Z. Lan, Impact of pH Value and Temperature on Cement-Based Materials Adsorbing Heavy Metal Ions, Mater. Sci. Forum. Trans Tech Publications Ltd., 2016, p. 265.
[36] R. Dariani, A. Esmaeili, A. Mortezaali, S. Dehghanpour, Photocatalytic reaction and degradation of methylene blue on TiO2 nano-sized particles, Optik 127 (2016) 7143–7154.
[37] J. Rahchamani, H.Z. Mousavi, M. Behzad, Adsorption of methyl violet from aqueous solution by polyacrylamide as an adsorbent: isotherm and kinetic studies, Desalination 267 (2011) 256–260.
[38] L. Ai, C. Zhang, Z. Chen, Removal of methylene blue from aqueous solution by a solvothermal-synthesized graphene/magnetite composite, J. Hazard Mater. 192 (2011) 1515–1524.
[39] G.Z. Kyzas, N.A. Travlou, O. Kalogirou, E.A. Deliyanni, Magnetic graphene oxide: effect of preparation route on reactive black 5 adsorption, Materials 6 (2013) 1360–1376.
[40] Z. Derakhshan, M.A. Baghapour, M. Ranjbar, M. Faramarzian, Adsorption of methylene blue dye from aqueous solutions by modified pumice stone: kinetics and equilibrium studies, Health Scope 2 (2013) 136–144.
[41] P. Monash, G. Pugazhenthi, Investigation of equilibrium and kinetic parameters of methylene blue adsorption onto MCM-41, Kor. J. Chem. Eng. 27 (2010) 1184–1191.
[42] P. Luo, B. Zhang, Y. Zhao, J. Wang, H. Zhang, J. Liu, Removal of methylene blue from aqueous solutions by adsorption onto chemically activated halloysite nanotubes, Kor. J. Chem. Eng. 28 (2011) 800–807.
[43] O. Amrhar, H. Nassali, M. Elyoubi, Adsorption of a cationic dye, methylene blue, ontoMoroccan illitic clay, J. Mater. Environ. Sci. 6 (2015) 3054–3065.
[44] A.B. Albadarin, C. Mangwandi, Mechanisms of Alizarin Red S and Methylene blue biosorption onto olive stone by-product: isotherm study in single and binary systems, J. Environ. Manag. 164 (2015) 86–93.
[45] H.H. Hammud, L. Fayoumi, H. Holail, E.-S.M. Mostafa, Biosorption studies of methylene blue by Mediterranean algae Carolina and its chemically modified forms. Linear and nonlinear models' prediction based on statistical error calculation, Int. J. Chem. 3 (2011) 147.
[46] L. Cui, Y. Wang, L. Gao, L. Hu, L. Yan, Q. Wei, B. Du, EDTA functionalized magnetic graphene oxide for removal of Pb (II), Hg (II) and Cu (II) in water treatment: adsorption mechanism and separation property, J. Chem. Eng. 281 (2015) 1–10.